

Middle Fusion and Multi-Stage, Multi-Form Prompts for Robust RGB-T Tracking

Qiming Wang^a, Yongqiang Bai^{a,*} and Hongxing Song^b

^aNational Key Lab of Autonomous Intelligent Unmanned Systems, Beijing Institute of Technology, Beijing 100081, China

^bNorth Lianchuang Communication Company, Jiangxi 600363, China

ARTICLE INFO

Keywords:

RGB-T tracking
Deep learning
Multi-modal fusion
Prompt learning

ABSTRACT

RGB-T tracking, a vital downstream task of object tracking, has made remarkable progress in recent years. Yet, it remains hindered by two major challenges: 1) the trade-off between performance and efficiency; 2) the scarcity of training data. To address the latter challenge, some recent methods employ prompts to fine-tune pre-trained RGB tracking models and leverage upstream knowledge in a parameter-efficient manner. However, these methods inadequately explore modality-independent patterns and disregard the dynamic reliability of different modalities in open scenarios. We propose M3PT, a novel RGB-T prompt tracking method that leverages middle fusion and multi-modal and multi-stage visual prompts to overcome these challenges. We pioneer the use of the middle fusion framework for RGB-T tracking, which achieves a balance between performance and efficiency. Furthermore, we incorporate the pre-trained RGB tracking model into the framework and utilize multiple flexible prompt strategies to adapt the pre-trained model to the comprehensive exploration of uni-modal patterns and the improved modeling of fusion-modal features, harnessing the potential of prompt learning in RGB-T tracking. Our method outperforms the state-of-the-art methods on four challenging benchmarks, while attaining 46.1 fps inference speed.

1. Introduction

Visual object tracking is a fundamental task in the computer vision community, which aims to continuously predict the state of a given target in every frame of a video sequence. It has a wide range of applications in fields such as autonomous driving [1], robot perception [2], and intelligent surveillance [3]. However, the tracking methods based on visible modality (also known as RGB tracking) are not robust in challenging scenarios such as extreme illumination and adverse weather, where the visible image quality is poor. To solve this problem, researchers have developed RGB-T tracking methods, which use the complementary information between thermal infrared and visible modalities to achieve all-weather and all-day tracking.

RGB-T tracking data has a complex and rich cross-modal feature space, which is a correlated combination of the two modal feature spaces rather than a simple addition. Since the data of the two modalities are synchronized in time and space, they share multiple patterns such as object boundaries, partial fine-grained information, etc.; however, due to the different imaging bands, they also have many modality-specific and discriminative patterns. These patterns form the key information in the feature space, and exploring, integrating, and utilizing them is essential for robust RGB-T tracking. To achieve this goal, many excellent works [4, 5, 6, 7, 8, 9, 10, 11, 12, 13, 14, 15] have proposed various effective fusion-based multi-modal tracking frameworks. These frameworks can be classified into three categories based on the fusion location: image-level, feature-level, and decision-level fusion frameworks, as shown in Figure 1(a)-(c). The image-level fusion framework is simple and efficient, but

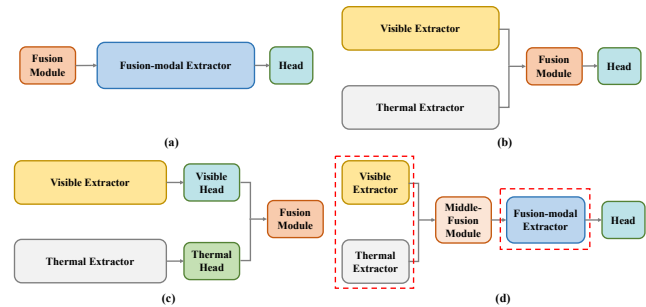


Figure 1: Comparison of different fusion tracking frameworks. (a)-(c) are the three mainstream frameworks: image-level, feature-level, and decision-level multi-modal fusion tracking frameworks, respectively. (d) is our proposed mid-term fusion tracking framework. Our framework, unlike the other three, splits the backbone into dual-stream and single-stream structures for uni-modal and fusion-modal feature representation, respectively, with the fusion module situated between them.

it does not exploit the two modalities separately, leading to poor performance. On the other hand, the feature-level and decision-level fusion frameworks extract rich features from both modalities, achieving high performance, but they introduce redundant computations due to the dual-stream architecture, which reduces the inference efficiency. Therefore, a natural question arises: can we design a framework that optimizes both performance and efficiency?

Inspired by this idea, we develop a middle fusion framework for RGB-T tracking, as shown in Figure 1(d). We place the fusion module in the middle of the backbone, and split the backbone into two parts: the pre-fusion backbone extracts the information of the two modalities independently, and the post-fusion backbone enhances the fusion-modal

*Corresponding author

✉ byfengyun@bit.edu.cn (Y. Bai)

features. By choosing an appropriate fusion location, this mixed-stream framework structure can achieve effective uni-modal modeling, as well as reduce the redundant feature extraction process, thus achieving the optimal balance between performance and efficiency. To the best of our knowledge, this is the first time that the middle fusion framework has been introduced into the RGB-T tracking task.

Another major focus of current research is how to address the data scarcity problem. The high cost of data acquisition leads to a persistent lack of sufficient annotated training data for the RGB-T tracking task, which severely hinders the data-driven model from learning reliable task-specific knowledge. Since most RGB-T tracking methods are derived from upstream methods, some studies use pre-trained upstream models to initialize the parameters and facilitate faster and better convergence of the current model. However, these full fine-tuning methods require tuning a large number of parameters, which imposes extremely high demands on the computing and storage capabilities of the device, and may cause overfitting and forgetting of upstream knowledge.

Considering these issues, some recent works [16, 17] introduce prompt learning into RGB-T tracking to better leverage the inheritance between upstream and downstream. With only tuning a small number of additional parameters, these methods can effectively reduce the gap between upstream and downstream tasks, and the training cost is much lower than the full fine-tuning methods. However, existing prompt-based methods have several key limitations: (i) Through direct or indirect image-level fusion, these methods hardly exploit any independent information within the modality, resulting in insufficient exploration and utilization of the discriminative patterns within the modality. (ii) They treat thermal infrared modality as an extra information only for generating prompts, and neglect the dynamic complementarity of the two modalities in open scenarios, thus failing to fully leverage the advantages of RGB-T tracking. (iii) They generate and inject prompts in a single manner.

Motivated by the previous discussions, our goal is to employ adaptable visual prompts to fine-tune the pre-trained upstream model to identify and leverage the distinctive and supplementary information within multi-modal features, thus optimizing the performance of RGB-T prompt tracking. For this purpose, we introduce four innovative visual prompt strategies to transfer the upstream knowledge to the middle fusion tracking framework. Consequently, we devise an effective and efficient RGB-T prompt tracking method with middle fusion and multi-stage, multi-form prompts (M3PT). In the method, we divide the backbone of the foundation model into two parts, each for one of the two modeling stages of the middle fusion framework. To adapt the first part to uni-modal exploration, we design a Uni-modal Exploration Prompt Strategy, which uses the first part backbone and some lightweight prompts UEP to explore the modality-shared and modality-independent patterns layer by layer, and further generates reliable intra-modal and inter-modal prompts to guide the subsequent layers to model key features

of the current modality and different modalities. Considering the dynamic complementarity of different modalities in open scenarios, we design a Middle Fusion Prompt Strategy to achieve adaptive selection and complementary fusion of the discriminative features of the two modalities, and use the fusion-modal features as natural prompts, which are fed into the second-stage backbone. To better adapt the backbone to the fusion-modal feature modeling, we design a Fusion-modal Enhancement Prompt Strategy, which guides the backbone to extract sufficient global and local fusion features, and thus obtain a richer fusion modality representation. Motivated by VPT, we design a Stage-aware and Modality-aware Prompt Strategy, which generates multiple learnable prompts to store the modality-fixed patterns and prepend them to the input of each stage. This strategy provides clear modality and stage indicators for the backbone. Notably, our method only contains 0.88M fine-tuning parameters. On four large-scale benchmarks, our method surpasses current state-of-the-art prompt-based methods by more than 2 percentage points on all metrics, and achieves competitive performance among existing methods. Moreover, our model has an inference speed of 46.1fps, exceeding most state-of-the-art methods. These results demonstrate the excellent balance of the proposed middle fusion framework in terms of performance and efficiency. Our work has the following main contributions:

(1) We propose a middle fusion framework for RGB-T tracking task for the first time, which is flexible and achieves a good balance between performance and efficiency compared to previous RGB-T tracking frameworks.

(2) Based on the proposed middle fusion framework, we develop a novel RGB-T prompt tracking method with multi-form and multi-stage visual prompts (M3PT), which fully unleashes the great potential of RGB-T prompt tracking through four flexible novel visual prompt strategies.

(3) Extensive experiments on four challenging RGB-T tracking benchmarks validate the effectiveness, efficiency, and parameter-efficiency of our method.

2. Related Work

2.1. RGB-T Tracking

In recent years, many excellent works [18, 19, 20, 21, 22, 23, 24, 25, 26, 27, 28, 29, 30, 31] have been produced on RGB object tracking. However, these methods are limited by the low image quality of visible modality in some challenging scenarios such as illumination changes, extreme lighting, and adverse weather, failing to meet the application requirements of tracking methods in open scenarios. Therefore, researchers have proposed and attracted widespread attention to RGB-T tracking, which utilizes the complementarity of visible and thermal infrared modalities to achieve all-weather tracking.

Lu et al. [8] employ diverse adapters to capture the intra-modal and inter-modal relation of different modalities, and propose a new loss function that reduces the distribution divergence of multi-modal features across layers. Zhang et

al. [9] develop a late fusion method that achieves robust multi-modal fusion through global and local weights, and uses Kalman filtering for motion estimation, to exploit the joint appearance and motion cues. Zhang et al. [10] extend the structure of siamese-like RGB trackers and introduce a weight generation model to enable the selection of unimodal discriminative features and the interaction of bimodal discriminative features. Tu et al. [7] propose a novel multi-modal multi-margin metric learning framework for RGB-T tracking, which preserves the relations of multilevel hard samples during training. A major challenge for data-driven models in RGB-T tracking is the scarcity of labeled training data, which results from the high cost of data collection, alignment, and annotation. Compared to the abundant training data [32, 33, 34] for RGB tracking task, the training data [35, 15] for RGB-T tracking is severely inadequate for learning sufficient task-relevant knowledge.

To address the problem of insufficient task data, some researchers propose attribute-based methods [6, 12, 13], which configure lightweight branches for each attribute to model the target appearance under these attributes, and then fuse these appearance features. During the training phase, these methods select sequences of each attribute from the training set to train the corresponding branches, thereby reducing the model's dependence on the training data to some extent. However, these methods have a tedious training process, and could not cover all the challenging attributes, while the excessive number of branches also limit their inference speed.

Meanwhile, some other works initialize the proposed RGB-T tracking models with RGB tracking models pre-trained on RGB tracking datasets, to guide the fast convergence of the models on limited training data. Zhang et al. [14] design a fusion module that can reduce the modality discrepancy and select the discriminative features, and initialize the RGB branch parameters with pre-trained DiMP parameters. Zhang et al. [15] integrate image-level, feature-level, and decision-level fusion into a unified framework, and use pre-trained DiMP model for parameter initialization. However, this approach requires a large number of parameters to be fine-tuned, which might cause the upstream knowledge to be forgotten during training, and also impose a heavy computational burden on the devices. To tackle this issue, some recent studies introduce the idea of prompt learning into RGB-T tracking, to achieve parameter-efficient fine-tuning and effective knowledge transfer from upstream tasks. We will introduce these methods in the next subsection.

2.2. Visual Prompt Learning

Prompt learning, as a parameter-efficient fine-tuning method, is originally proposed in the natural language processing field for transferring large language models to downstream tasks. Recently, this idea is introduced to the computer vision field [36, 37, 38, 39], using a small amount of image data from downstream tasks to generate effective visual prompts for transferring pre-trained models. Jia et al. [36] use a small number of learnable parameters as visual

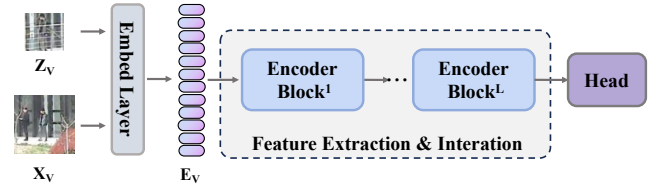


Figure 2: The tracking pipeline of the RGB-based foundation model. The foundation model is a one-stream one-stage RGB tracker based on transformer backbone. The subscript V denotes the visible modality, and the superscript i denotes the layer number of the Transformer Encoder Block.

prompts, and prepend them to the input sequences of each layer. Bar et al. [37] propose to use the input-output pairs of downstream task examples and a new input image concatenated as visual prompts, to make the model learn to fill in the gaps, thus formulating this problem as an image inpainting problem. Considering that the downstream image datasets sometimes have large distribution differences, Huang et al. [38] cluster the image datasets into multiple subsets with the same internal distribution, configure unique prompts for each subset, and initialize them with a meta-prompt.

Yang et al. [16] take the weighted addition of two modal images as visual prompts and feed the prompts into the pre-trained RGB tracking model, which is the first time that prompt learning is introduced into the multi-modal tracking task. Zhu et al. [17] formulate the multi-modal tracking task as an RGB tracking task with an auxiliary modality input, and design a lightweight prompter to generate visual prompts from the auxiliary modality data. However, to bridge the gap between the upstream and downstream tasks, these methods overemphasize the role of the RGB modality, neglecting the dynamic dominance difference of different modalities in various scenarios, and thus fail to exploit modality-independent clues. In contrast, our method achieves effective exploration and adaptive fusion of different modality features by using more flexible and diverse prompt strategies, and therefore performs more robust when facing various challenging scenarios.

3. Preliminaries

Before presenting our RGB-T tracking method, we first define the RGB tracking task and briefly review the foundation model. For more details, please refer to OSTRack [27].

The RGB object tracking task aims to estimate the bounding box B of the target in each frame, given the bounding box B_0 of the target in the initial frame of a video sequence. The mainstream RGB tracking methods formulate this task as a similarity matching problem between the template image $I_{V,Z} \in R^{H_Z \times W_Z \times C}$ from the initial frame and the search region $I_{V,X} \in R^{H_X \times W_X \times C}$ from the current frame, where V denotes the visible modality, and X and Z denote the search and template respectively. Therefore, the tracking task can be expressed as $B = Track(I_{V,Z}, I_{V,X})$, where $Track()$ denotes the tracker function.

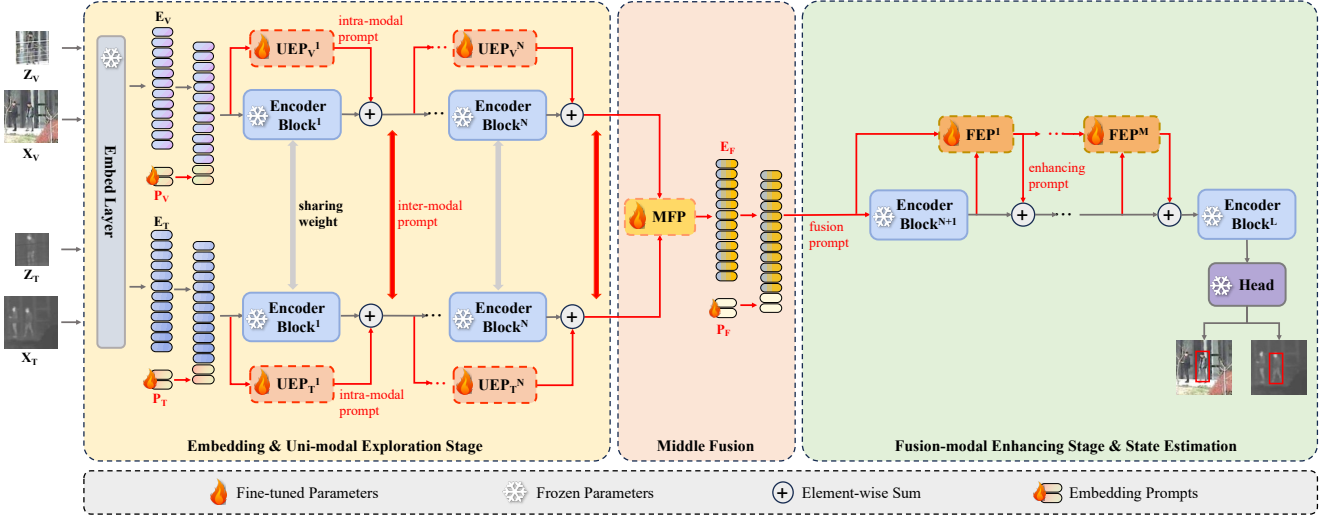


Figure 3: Pipeline of our M3PT. In this method, two modal images of the same size go through five steps: embedding, uni-modal exploration, middle fusion, fusion-modal enhancing, and state estimation, to obtain the predicted bounding box. Here, the L transformer encoder blocks from the upstream model are divided into two groups, for the uni-modal exploration and fusion-modal enhancing modeling stages respectively. The subscripts and superscripts of the modules and symbols indicate the modality and the layer number respectively.

As shown in Figure 2, we choose a one-stream one-stage RGB tracking model 2 as our foundation model. Built on ViT [40], the method is one-stream one-stage, which means that the feature extraction and template-search interaction are performed simultaneously by a single transformer backbone. The model consists of an embedding layer, a backbone composed of L transformer encoder blocks stacked together, and a head network. The embedding layer maps the input template and search images into 16×16 patches, reshapes them to $1D$ tokens and concatenates them as $E_V^0 = [E_{V,Z}^0; E_{V,X}^0] \in R^{(N_Z + N_X) \times D}$, where N_Z and N_X respectively denote the number of template tokens and search tokens and D denotes the dimension of the tokens. Then, the encoder blocks $\{Encoder^l, l \in (1, L)\}$ perform self-attention mechanism [41] on the concatenated tokens E_V^0 , thus achieving joint feature extraction and interaction between the template and the search:

$$E_V^L = Encoder^L(\dots Encoder^2(Encoder^1(E_V^0))) \quad (1)$$

where superscripts represent the number of layers.

Finally, the search tokens that fully interact with the template are separated from the E_V^L by unconcatenation, and are reshaped by the head network into features $F_{V,X} \in R^{H_X \times W_Z \times C}$ for the target state estimation:

$$F_{V,Z}, F_{V,X} = \text{reshape}(\text{unconcaten}(E_V^L)) \quad (2)$$

$$B = \text{Head}(F_{V,X}) \quad (3)$$

4. Methodology

4.1. Overview

In this work, we propose a novel RGB-T prompt tracking method M3PT that leverages a middle fusion tracking framework and multi-form, multi-stage visual prompts. The overall pipeline of our method is shown in Figure 3.

We first developed a multi-modal tracking framework based on middle fusion. The framework's backbone consists of two parts for different stages. The first-stage backbone is a dual-stream network that extracts two uni-modal features separately. The second-stage backbone is a single-stream network that enhances the fusion-modal features. The middle fusion module is inserted between the two backbone stages.

Furthermore, we embed the pre-trained foundation model into our framework by using four flexible prompt strategies to achieve effective knowledge transfer. These strategies are: (1) The L transformer encoder blocks from the foundation model backbone are divided into two groups, containing N and M encoder blocks respectively, for feature extraction in two stages. (2) The Uni-modal Exploration Prompt Strategy extends the first-group encoder blocks into a parameter-sharing dual-branch structure, and configures the designed UEP in parallel with them layer by layer, to explore the modality-independent information and generate intra-modal and inter-modal prompts, thus better adapting the encoder blocks to uni-modal feature modeling. (3) The Middle Fusion Prompt Strategy inserts the designed MFP after the first-stage backbone, and feeds the fusion-modal features output by MFP as visual prompts to the backbone in the later stage, to adapt it to the fusion-modal modeling. (4) The Fusion-modal Enhancing Prompt Strategy configures a lightweight prompter FEP in parallel with the second-stage backbone layer by layer, to obtain a richer fusion-modal feature representation and enhance the fusion-modal features propagated forward in the backbone. (5) The Modality-aware and Stage-aware Prompt Strategy prepends three learnable prompts to the input of the backbones in two stages, respectively, to guide them to identify the distribution characteristics of the current modality faster. (6) The head

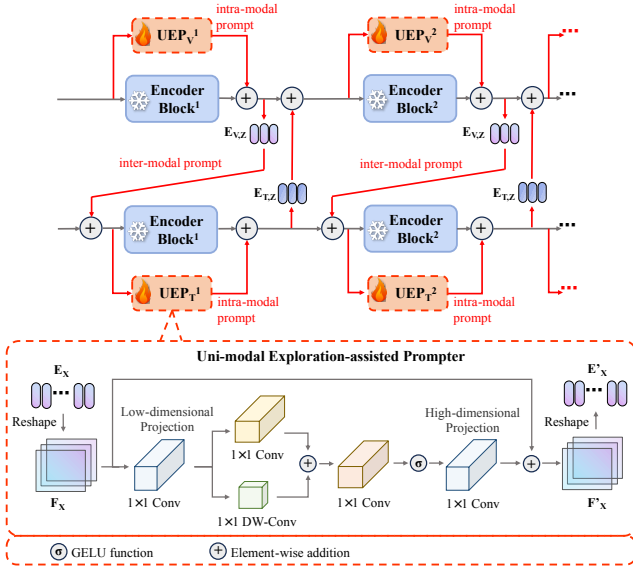


Figure 4: The pipeline of our Uni-modal Exploration Prompt Strategy and overall architecture of our designed Uni-modal Exploration-assisted Prompter (UEP). The modality-independent information extracted by the UEP is firstly added to the output of the encoder block of the same modality as intra-modal prompts, and the prompted template tokens are injected as inter-modal prompts in an asymmetric cross-layer manner.

network of the foundation model is directly used to estimate the target state on the search features.

4.2. Uni-modal Exploration Prompt Strategy

Previous prompt tracking methods hardly exploited any modality-independent information, resulting in insufficient mining and utilization of the discriminative patterns within the modality. To address this issue, we propose a Uni-modal Exploration Prompt Strategy and design a lightweight Uni-modal Exploration-assisted Prompter UEP, to prompt the first-stage backbone to explore and model the uni-modal features.

The proposed UEP is shown in Figure 4. The input tokens E_X are first reshaped into features and mapped to a low-dimensional feature space. Then, we configure parallel 1×1 convolutional layer and DW convolutional layer to explore modality-independent channel correlation features through different channel combinations, and subsequently use a 1×1 convolutional layer with activation function GELU to achieve local feature extraction. Finally, the features are remapped to the high-dimensional space. In addition, UEP configures residual connection. Since the feature extraction process is all performed in the low-dimensional space, each UEP contains only a small number of learnable parameters. In our case, we set the dimensions of the low-dimensional feature space of the UEP for the thermal infrared and visible modalities to 8 and 16, respectively, to explore the modality-independent feature representation of the two modalities as much as possible.

Furthermore, to utilize the information to enhance intra-modal discriminative features and achieve effective inter-modal interaction, we generate two kinds of visual prompts based on the output of UEP: intra-modal prompts and inter-modal prompts. Specifically, (1) we add the modality-independent features extracted by UEP as intra-modal prompts to the modality-shared features output by Encoder Block, thus providing a richer uni-modal representation for the next layer of backbone, as shown in Figure 4, taking the visible branch as an example, this hint process can be expressed as:

$$P_{V,intra}^n = UEP_V^n(H_V^n) \quad (4)$$

$$E_V^n = Encoder^n(H_V^n) + P_{V,intra}^n \quad (5)$$

where subscript V denotes visible modality, superscript n denotes layer number, H denotes input tokens of an encoder block. (2) We separate the template tokens from the prompted modal features $E_V^n \in R^{(N_Z+N_X) \times D}$, and use them as inter-modal prompts to add element-wise with the template of another modality, as shown in Figure 4. We adopt an asymmetric cross-layer manner to inject the prompts, specifically, we inject the inter-modal prompts from the thermal infrared modality into the input of visible modality branch at the same layer, and inject the intra-modal prompts from visible modality into the input of thermal infrared modality branch at the next layer:

$$[E_{V,Z}^n, E_{V,X}^n] = unconcaten(E_V^n) \quad (6)$$

$$P_{V,inter}^n = E_{V,Z}^n \quad (7)$$

$$H_{T,Z}^{n+1} = E_{T,Z}^n + P_{V,inter}^n \quad (8)$$

$$[E_{V,Z}^n, E_{V,X}^n] = unconcaten(E_V^n) \quad (9)$$

$$P_{V,inter}^n = E_{V,Z}^n \quad (10)$$

$$H_{T,Z}^{n+1} = E_{T,Z}^n + P_{V,inter}^n \quad (11)$$

where $unconcaten()$ refers unconcatenation. The reason for using template features as inter-modal prompts is that the templates contain less background noise and more clues about the target appearance. Therefore, by using inter-modal prompts, we provide the upstream backbone with more modality-complementary target appearance clues, which enables the feature extraction of upstream backbone to focus more on the potential regions of the target.

4.3. Middle Fusion Prompt Strategy

To achieve adaptive fusion of the uni-modal features extracted by the first-stage backbone and provide reliable fusion task prompts for the second-stage backbone, we propose a Middle Fusion Prompt Strategy that utilizes our designed middle fusion prompter MFP to perform adaptive selection of discriminative features and complementary fusion, and views the fusion-modal features as natural visual prompts for the next stage.

MFP is shown in Figure 5. The input feature tokens of the two modalities E_V and E_T are first reshaped into features F_V and F_T , and then mapped to low-dimensional feature space by two weight-unshared 1×1 convolutional

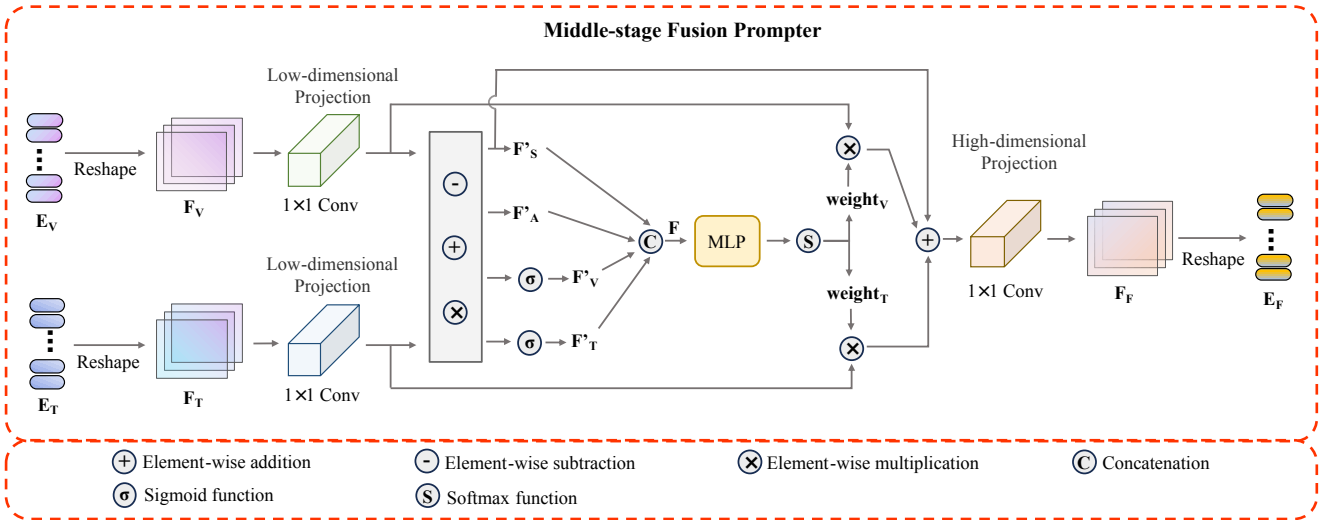


Figure 5: Overall structure of our designed Middle Fusion Prompter (MFP).

layers, respectively. Here, we set the dimensions of the low-dimensional feature space of the MFP to 16. Then, inspired by [42], we separate the modality-shared and modality-independent information extracted at each element:

$$F'_S = (F_{V,L} \times F_{T,L}) \quad (12)$$

$$F'_A = (F_{V,L} + F_{T,L}) \quad (13)$$

$$F'_V = \text{Sigmoid}(F_{V,L} - F_{T,L}) \quad (14)$$

$$F'_T = \text{Sigmoid}(F_{T,L} - F_{V,L}) \quad (15)$$

where $F_{V,L}$ and $F_{T,L}$ represent the visible light and infrared features mapped to the low-dimensional space, respectively, F'_S represents the modality-shared features, F'_A represents the overall features, F'_V and F'_T represent the visible light and infrared modality-independent features, respectively, \times , $+$, and $-$ represent element-wise multiplication, addition, and subtraction, respectively, and sigmoid operation is used to enhance the local modality-independent features. After that, we concatenate these features in the following order and generate adaptive discriminative filtering weights based on them:

$$F = \text{concaten}(F'_V, F'_S, F'_A, F'_S, F'_T) \quad (16)$$

$$[weight_V, weight_T] = \text{Softmax}(fc(F)) \quad (17)$$

where $fc()$ denotes fully connected layer and $\text{concaten}()$ denotes concatenation. And the adaptive discriminative fusion process is expressed as follows:

$$F_{F,L} = F'_S + F_{V,L} \times weight_V + F_{T,L} \times weight_T \quad (18)$$

It is noteworthy that we add the shared features F'_S on top of the weighted fusion, considering that the useful information that may exist at the low-weight positions in the discriminative fusion process will be suppressed, and these low-weight information mostly belong to the modality-shared information. Previous weighted fusion methods have

ignored it. Therefore, we ensure the integrity of the effective information by adding F'_S . Finally, the fused features are remapped to the original dimension and reshaped into tokens.

We propose a Middle Fusion Prompt Strategy that inserts MFP after the first-stage backbone, which contains N Encoder Blocks. Unlike [16] and [17], which only perform image-level weighted fusion of the two modal features, we perform adaptive and discriminative selection and complementary fusion of the two modal features that have been fully explored and modeled, and we retain as much useful information as possible. Therefore, the obtained fusion-modal features can serve as reliable fusion-modal prompts injected into the second-stage upstream backbone, making it better adapt to the fusion-modal modeling task.

To the best of our knowledge, this is the first time that the middle fusion framework is introduced to the RGB-T tracking task. Compared with the tracking framework based on image-level fusion, our framework can more effectively explore the independent information of the two modalities; compared with the tracking framework based on feature-level fusion and decision-level fusion, our method can effectively compress the redundant modeling computation and reduce the model parameters. While keeping the total amount of backbone parameters from the pre-trained model unchanged, by flexibly adjusting the proportion allocation of the two-stage backbone parameters, our method can achieve the optimal balance between performance and efficiency.

4.4. Fusion-modal Enhancing Prompt Strategy

To further narrow the gap between the second-stage modeling and the upstream modeling, we propose a Fusion-modal Enhancing Prompt Strategy, which introduces the fusion-modal enhancing prompter FEP to provide enhanced prompts for the fusion-modal features. Here, FEP adopts the same structure as MCP in [17], and is also configured in parallel with encoder blocks layer by layer, as shown in

Figure 3. But unlike [17], our second-stage backbone input is a single-stream fusion features, which serves as one of the input streams of the first-layer FEP, and the output of the first-layer Encoder Block serves as another input stream of the first-layer FEP. And the output of FEP serves as the visual cue for self-enhancement and one of the input streams of the next-layer FEP, which can be expressed as:

$$P^m = FEP^{m-N}(H^m, Encoder^m(H^m)), m = N + 1 \quad (19)$$

$$P^m = FEP^{m-N}(P^{m-1}, Encoder^m(H^m)), m > N + 1 \quad (20)$$

$$H^{m+1} = Encoder^m(H^m) + P^m, m > N + 1 \quad (21)$$

By using this quasi-residual connection method, the local key information of the fusion-modality is enhanced and injected into the next layer, providing a more rich and reliable fusion-modal feature representation, which makes the subsequent upstream backbone adapt to the fusion-modal modeling.

4.5. Modality-aware And Stage-aware Prompt Strategy

We intuitively assume that each modality contains some fixed patterns such as low-level distribution characteristics, which can be learned and stored to guide the backbone to quickly and familiarize themselves with the current modality and modeling task. Therefore, we propose a Modality-aware and Stage-aware Prompt Strategy that uses three learnable prompts to learn and store the fixed patterns of the visible light, infrared, and fusion modalities. Inspired by [36], we prepend these prompts to the input of corresponding encoder blocks, to provide clear modality and stage identification for the upstream backbone, as shown in Figure 3.

These prompts only participate in the feature extraction of upstream backbone, and do not participate in the generation and other prompting processes. In other words, these prompts are separated from the total tokens at the input of all prompter branches, and are concatenated with the prompted feature tokens after completing the other prompting processes. Specifically, after MFP completes the fusion of the two modal features, the two separated uni-modal prompts are added to the fusion-modal prompts, and prepended to the input of the second-stage backbone. Since they do not contain positional encoding, these prompts can be inserted into any position of the feature tokens. In our case, we set the token number of the learnable prompts to 2.

4.6. Head, Loss and Training

The head network parameters of the base model are frozen and directly used in our framework to estimate the current state of the target. The loss function during training is also the same as the base model, including the weighted classification loss, GIoU loss, and L1 loss, whose formulas are as follows:

$$L = L_{cls} + \lambda_{iou} L_{giou} + \lambda_{L1} L_{L1} \quad (22)$$

Where λ_{giou} and λ_{L1} are exactly the same as the training settings of the foundation model.

5. Experiment

5.1. Experimental Settings

5.1.1. Implementation Details

We use the pre-trained OTrack-256 model as the foundation of our method. We fine-tune the prompt-related parameters that we designed on the LasHer's train split and freeze all the other parameters of the foundation model. We set the batch size to 32 and the number of epochs to 60. We use the AdamW optimizer with a weight decay rate of 0.0001 and an initial learning rate of 0.0004, which decays to 0.1 times the original value after 48 epochs. The training process is end-to-end. After the offline training, we do not perform any online parameter update operations which may reduce our model's inference speed. The template image size is set to 128×128 and the search image size is set to 256×256. The block number of the first-stage backbone is set to 2. We conduct all experiments on four Nvidia RTX 3090 GPUs, using Python and PyTorch.

5.1.2. Experimental Benchmarks

We evaluate the performance of our method on four public and challenging RGBT tracking benchmarks: LasHer [35], RGBT234 [43], RGBT210 [44], and VTUAV [15]. We will briefly describe them in the following paragraphs.

LasHer: LasHer is the largest-scale RGB-T tracking benchmark, containing 1224 highly aligned video sequence pairs and 734.8K image pairs. The benchmark covers 32 common object categories and 19 typical challenge attributes, posing great challenges for current RGB-T tracking algorithms.

RGBT210: RGBT210 consists of 210 video sequence pairs and 210K image pairs, with the longest video sequence having 8K frames.

RGBT234: RGBT234 is the extension of RGBT210, containing 234 RGBT video sequence pairs and 234K image pairs. The benchmark includes 12 common challenge attributes.

VTUAV: VTUAV is a large-scale benchmark, comprising 500 video sequence pairs and 1700K image pairs, with high resolution. It is divided into long-term subset and short-term subset, each containing 250 video sequences. VTUAV is the first RGB-T tracking benchmark that formally proposes the long-term tracking task.

5.2. Evaluation Results on LasHer

We evaluate the performance of our proposed method on LasHer, and compare it with 14 state-of-the-art RGB-T tracking methods. These methods fall into three categories: the first category consists of methods that use pre-trained RGB tracking models for prompt fine-tuning, containing M3PT, ViPT-deep[17], ViPT-shaw[17], and ProTrack[16]; the second category comprises methods that use pre-trained RGB tracking models for full fine-tuning, containing ECMD[42], MFNet[14], HMFT[15], mfDiMP[5], and SGT++[43]; the

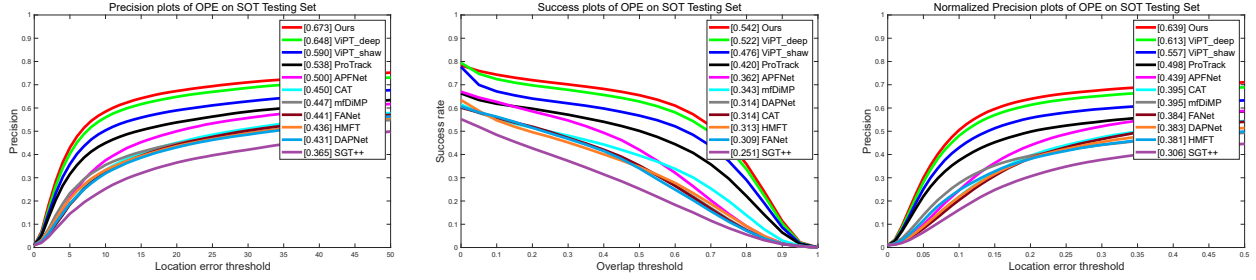

Figure 6: The evaluation curves of the three metrics PR, SR, and NPR on LasHer.

Table 1

The overall performance on LasHer. The red, blue, and green fonts indicate the first, second, and third places of each evaluation metric, respectively.

	Type	PR↑	NPR↑	SR↑	Speed↑
M3PT	Prompt fine-tune	67.3	63.9	54.2	46.1fps
ViPT-deep[17]	Prompt fine-tune	64.8	61.3	52.2	-
ViPT-shaw[17]	Prompt fine-tune	59.0	55.7	47.6	-
ProTrack[16]	Prompt fine-tune	53.8	49.8	42.0	-
ECMD[42]	Full fine-tune	59.0	54.6	46.4	30.0fps
MFNet[14]	Full fine-tune	59.7	55.4	46.7	18.0fps
HMFT[15]	Full fine-tune	43.6	38.1	31.3	25.1fps
mfDiMP[5]	Full fine-tune	44.7	39.5	34.3	22.0fps
SGT++[43]	Full fine-tune	36.5	30.6	25.1	1.2fps
PLASSO[45]	Other	54.7	-	47.2	-
APFNet[13]	Other	50.0	43.9	36.2	1.9fps
MANet++[8]	Other	46.7	40.8	31.7	16.1fps
CAT[6]	Other	45.0	39.5	31.4	-
FANet[46]	Other	44.1	38.4	30.9	12.0fps
DAPNet[47]	Other	43.1	38.3	31.4	-

third category includes methods that do not use pre-trained upstream parameters, containing APFNet[13], MANet++[8], FANet[46], PLASSO[45], CAT[6], and DAPNet[47]. The evaluation metrics used by LasHer are prediction accuracy (PR), normalized prediction accuracy (NPR), and success rate (SR).

Table 1 shows the evaluation results of all methods on LasHer. Our proposed M3PT method achieves PR, NPR, and SR scores of 67.3, 63.9, and 54.2 respectively, which are 2.5, 2.6, and 2.0 percentage points higher than the current best prompt fine-tuning method ViPT-deep respectively. Our method's performance ranks first among all existing prompt fine-tuning methods. This demonstrates the superiority of our proposed method over the previous prompt methods. Moreover, our method also outperforms most other state-of-the-art methods, even including multiple fine-tune state-of-the-art methods. This indicates that our method further unleashes the huge potential of prompt fine-tuning in RGB-T tracking tasks through a reliable framework and multiple flexible prompt strategies. Furthermore, our method's inference speed reaches 46.1fps, proving the efficiency of our proposed middle fusion tracking framework. In addition, we also use the LasHer toolkit to plot the PR, NPR, and SR

evaluation curves of our method and 10 open-source state-of-the-art methods, as shown in Figure 6. Our method shows great competitiveness under all thresholds of each evaluation curve.

We notice that LasHer contains 19 classic challenge attributes and has been finely annotated, which can cover most complex scenarios in the real world. To evaluate the performance of our proposed method in these scenarios and further verify whether it can fully exploit the advantages of RGB-T tracking, we use the LasHer toolkit to plot per-attribute PR evaluation curves of our method and 10 other open-source methods under these 19 challenge attributes. The evaluation results are shown in Figure 7. Our method shows leading performance that far exceeds other similar methods on 18 challenge attributes (TO, TC, OV, SV, PO, NO, SA, MB, LI, HO, ARC, LR, CM, FM, HI, BC, IV, DEF), which include not only the common challenge attributes of visual tracking (TO, OV, SV, PO, NO, SA, MB, ARC, LR, CM, FM, BC, DEF), but also the challenge attributes that cause serious degradation of the reliability of the visible modality (LI, HI, AIV) and thermal infrared modality (TC). This proves that our method can indeed fully explore and

Middle Fusion and Multi-Stage, Multi-Form Prompts for Robust RGB-T Tracking

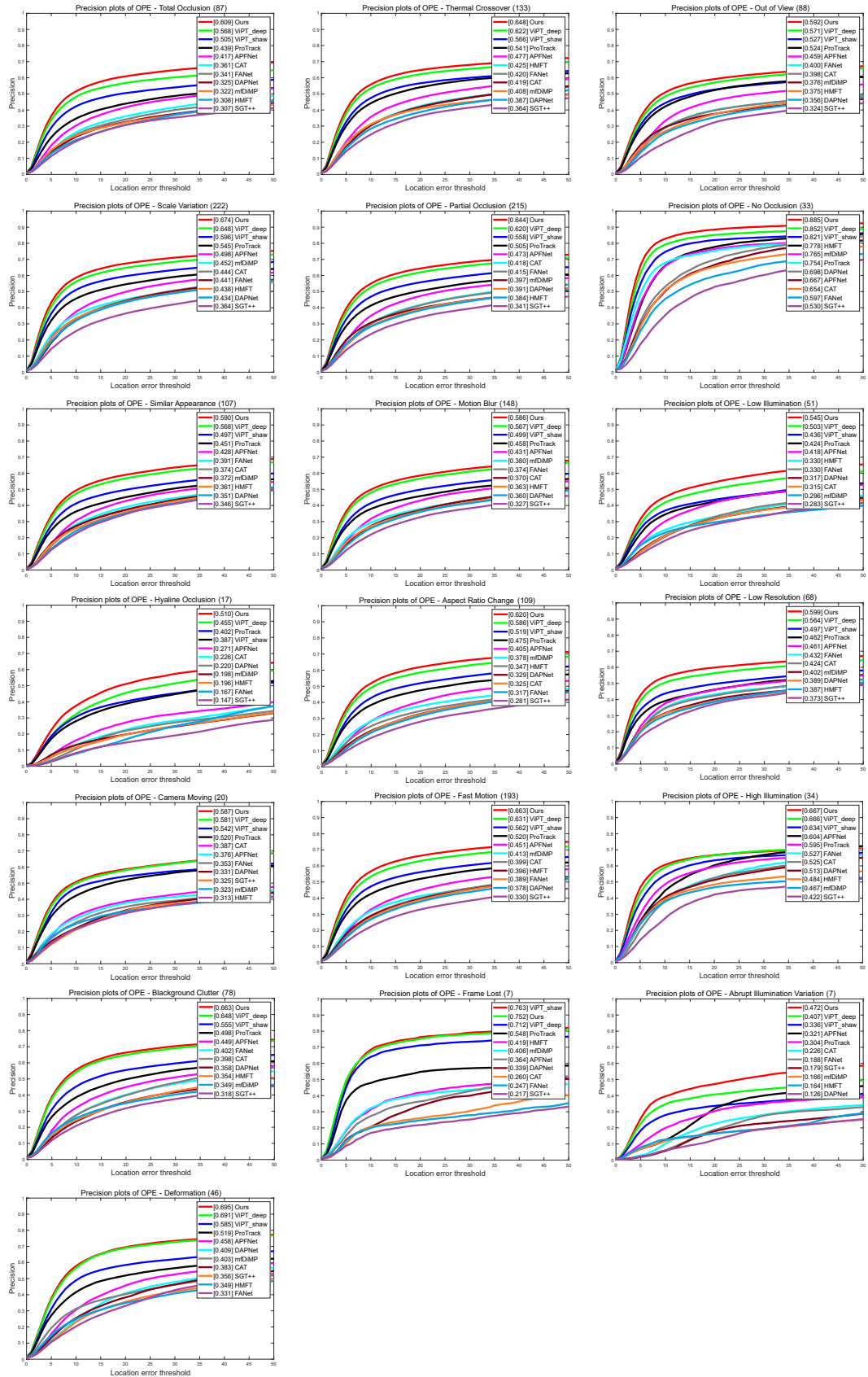


Figure 7: The evaluation curves of the MPR metric for the 19 annotated challenge attributes on LasHer.

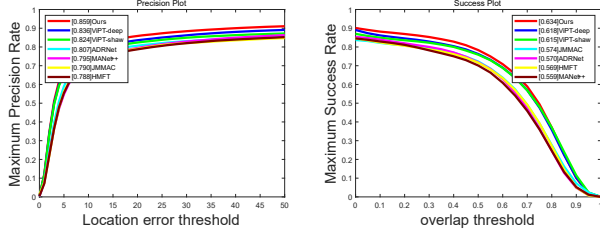


Figure 8: The evaluation curves of the two metrics MPR and MSR on RGBT234.

Table 2

The overall performance on RGBT234. The red, blue, and green fonts indicate the first, second, and third places of each evaluation metric, respectively.

	MPR \uparrow	MSR \uparrow	Speed \uparrow
M3PT	85.9	63.4	46.1fps
ECMD[42]	82.4	58.4	30.0fps
MFNet[14]	84.4	60.1	18.0fps
DMCNet[48]	83.9	59.3	2.2fps
ViPT-deep[17]	83.6	61.8	-
ViPT-shaw[17]	82.4	61.5	-
PLASSO[45]	82.7	59.2	-
APFNet[13]	82.7	57.9	1.9fps
LRMW[49]	82.5	61.6	24.6fps
MIRNet[50]	81.6	58.9	30.0fps
ADRNet[12]	80.7	57.0	25.0fps
MANet++[8]	79.5	55.9	16.1fps
M5L[7]	79.5	54.2	9.0fps
JMMAC[9]	79.0	57.4	-
HMFT[15]	78.8	56.9	25.1fps

utilize the key modes of modality sharing and modality independence, achieving robust tracking in various challenge scenarios.

5.3. Evaluation Results on RGBT234

On RGBT234, we compare our proposed method with 14 state-of-the-art methods, and the comparison results are shown in Table 2. According to Table 2, our method surpasses ViPT-deep by 2.3 and 1.6 percentage points on the MPR and MSR metrics respectively, and ranks first among all methods on all metrics and tracking speed. We also use RGBT234 toolkit and plot the MSR and MPR evaluation curves of our method and 6 open-source methods, as shown in Figure 8.

RGBT234 also provides annotations for 12 classic challenge attributes (CM, HO, FM, SV, PO, LI, NO, TC, BC, MB, DEF, LR). Therefore, we plot the per-attribute MPR evaluation curves, as shown in Figure 9. Our method shows leading performance on 10 of the 12 challenge attributes (CM, HO, FM, SV, PO, NO, TC, BC, DEF, LR), demonstrating the robustness and application potential of our method in open world scenarios.

Table 3

The overall performance on RGBT210. The red, blue, and green fonts indicate the first, second, and third places of each evaluation metric, respectively.

	PR \uparrow	SR \uparrow	Speed \uparrow
M3PT	83.9	60.8	46.1fps
ViPT-deep[17]	81.3	59.2	-
ViPT-shaw[17]	80.4	59.1	-
JMMAC[9]	78.3	55.3	-
ADRNet[12]	79.4	54.8	25.0fps
DMCNet[48]	79.7	55.5	2.2fps
CAT[6]	79.2	53.3	-
MANet++[8]	77.2	53.4	25.4fps
HMFT[15]	77.7	55.7	25.1fps

Table 4

The overall performance on VTUAV. The red and blue fonts indicate the first and second places of each evaluation metric, respectively.

	Long-term		Short-term		Speed \uparrow
	MPR \uparrow	MSR \uparrow	MPR \uparrow	MSR \uparrow	
M3PT	55.6	47.4	75.5	63.0	46.1fps
HMFT-LT[15]	53.6	46.1	-	-	8.1fps
HMFT[15]	41.4	35.5	75.8	62.7	25.1fps
FSRPN[51]	36.6	31.4	65.3	54.4	36.8fps
mfDiMP[5]	31.5	27.2	67.3	55.4	25.8fps
DAFNet[52]	25.3	18.8	62.0	45.8	7.1fps
ADRNet[12]	23.5	17.5	62.2	46.6	10.3fps

5.4. Evaluation Results on RGBT210

We compare our method with 8 state-of-the-art methods on RGBT210, and show the comparison results in Table 3. Our method achieves PR and SR scores of 83.9 and 63.8 respectively, surpassing ViPT-deep by 2.3 and 1.6 percentage points, and demonstrating its competitiveness among all methods. We plot the SR and PR evaluation curves of our method along with six leading open-source methods, as shown in Figure 10.

5.5. Evaluation Results on VTUAV

VTUAV is the first benchmark to propose a long-term tracking task, which poses new challenges for RGB-T tracking. The VTUAV test set consists of two subsets: long-term tracking subset and short-term tracking subset. We select six RGB-T tracking methods that have been evaluated on VTUAV and compare them with our method on both subsets. Table 4 shows the results. In addition, we use the VTUAV toolkit to plot the MPR and MSR evaluation curves of our method and other open-source state-of-the-art methods on the long-term tracking subset and the short-term tracking subset, respectively, as shown in Figure 11 and Figure 12.

The evaluation results and curves show that our method performed very competitively on both subsets. It is encouraging that, despite not introducing any model online update or template update operation in the inference stage, our

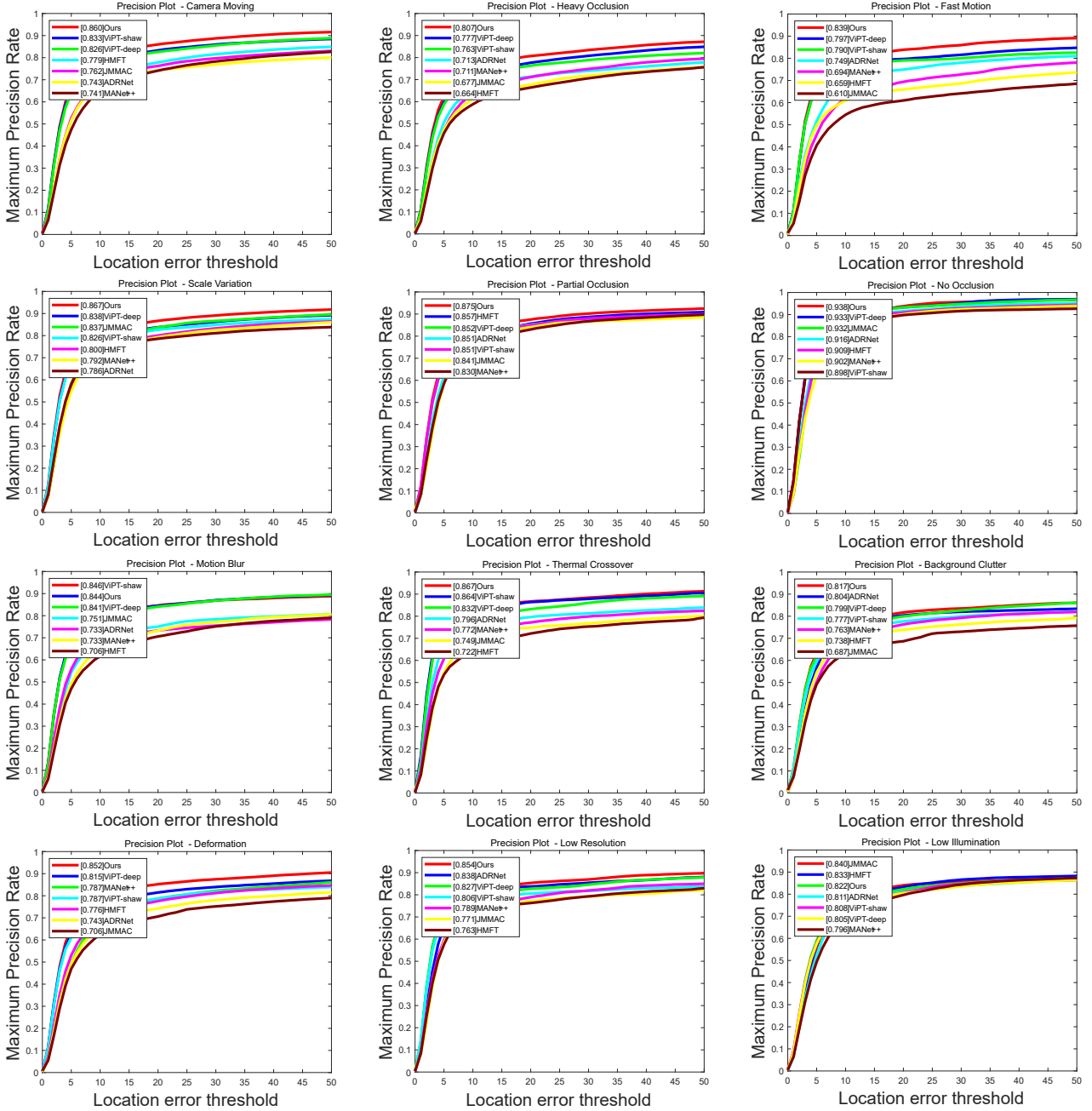


Figure 9: The evaluation curves of the MPR metric for the 12 annotated challenge attributes on RGBT234.

method still achieves state-of-the-art on the VTUAV long-term tracking test set. The second-ranked HMFT-LT method on the long-term subset, which introduces a model online update mechanism to adapt to the long-term tracking task, has an inference speed of only 8.1fps, less than one-fifth of the M3VPT inference speed. This is because our proposed method fully explores the complementary information of the dual modality and maximizes the use of upstream knowledge in the long-term tracking task, enabling it to better adapt to the more complex and open long-term tracking task.

5.6. Qualitative Analysis

We conducted a qualitative analysis of our proposed method on three video sequences from LasHer, namely rightbike, darktreesboy, and ab_rightlowerredcup_quezhen, which contain four of the most common challenging scenarios: low illumination and illumination variation, which degrade the reliability of the visible modality; similar appearance, which is a common challenge for tracking tasks; and temperature crossover, which degrades the reliability of the thermal infrared modality. We also compared our method with four state-of-the-art RGB-T tracking methods: ViPT-deep, ProTrack, APFNet and HMFT.

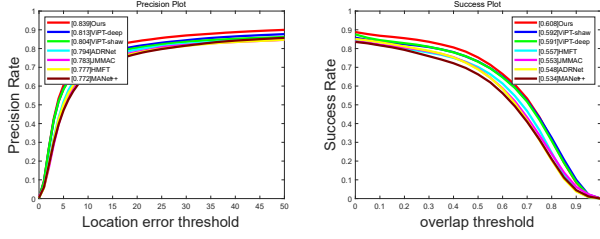


Figure 10: The evaluation curves of the two metrics PR and SR on RGBT210.

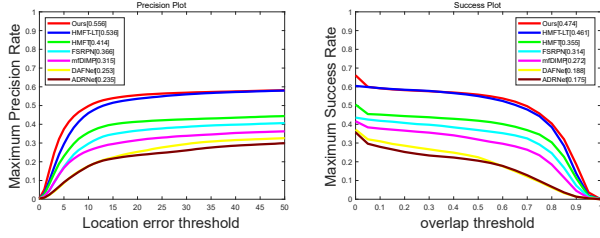


Figure 11: The evaluation curves of the two metrics MSR and MPR on the long-term test subset of VTUAV.

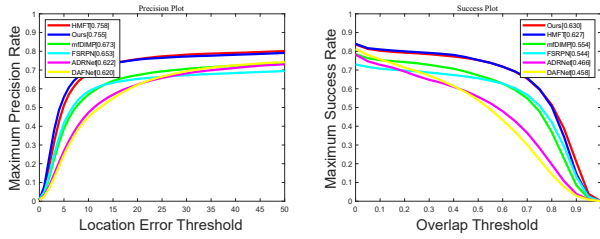


Figure 12: The evaluation curves of the two metrics MSR and MPR on the short-term test subset of VTUAV.

Figure 13 (a)-(d) shows the qualitative evaluation results. Our method's tracking results are the most stable and accurate in low illumination and illumination variation scenarios, fully exploiting the potential of RGB-T tracking. In the similar appearance scenario, our method can still accurately locate and estimate the target boundary, while other methods fail due to interference from similar objects. In the temperature crossover scenario, which is a unique challenge for RGB-T tracking, our method is clearly the closest to the ground truth. The qualitative test results demonstrate the high robustness of M3PT in various common challenging scenarios.

5.7. Parameters Comparison

We verify the parameter-efficiency and effectiveness of our proposed method by comparing it with the RGB tracking foundation model and two best prompt methods ViPT-deep and ViPT-shaw. Table 5 shows that our method adds only 0.88M extra parameters on the foundation model, which are the only parameters that need to be fine-tuned during training. Compared with ViPT-deep, our method adds only 0.04M parameters, but the evaluation results on LasHer show that our method surpasses ViPT-deep by 2.5 and 2.0 percentage points on the PR and SR metrics respectively.

Table 5

The comparison of the foundation model, two similar methods and our method in terms of parameter size and performance. SOT stands for the foundation model, Params represents the model's parameter size, and Tuned Params represents the number of parameters involved in fine-tuning.

	Params	Tuned Params	LasHer	
			PR \uparrow	SR \uparrow
SOT	92.12M	-	51.5	41.2
ViPT-shaw	92.73M	0.61M (0.66%)	59.0 (+7.5)	47.6 (+6.4)
ViPT-deep	92.96M	0.84M (0.91%)	64.8 (+13.3)	52.2 (+11.0)
M3PT	93M	0.88M (0.96%)	67.3 (+15.8)	54.2 (+13.0)

Table 6

The ablation experiment results. In the table, the four abbreviations represent the four prompting strategies. UEPS: Uni-modal Exploration Prompt Strategy, MFPS: Middle Fusion Prompt Strategy, FEPS: Fusion-modal Enhancing Prompt Strategy, MSPS: Modality-aware and Stage-aware Prompt Strategy.

	UEPS	MFPS	FEPS	MSPS	RGBT234	
					MPR \uparrow	MSR \uparrow
					63.5	48.3
✓					74.9	56.5
		✓			79.2	58.5
			✓		82.7	60.7
✓	✓		✓		84.5	62.2
✓	✓		✓	✓	85.9	63.4

The comparison result proves the parameter-efficiency and effectiveness of our method.

5.8. Ablation Study

Our proposed method consists of four prompt strategies: Uni-modal Exploration Prompt Strategy, Middle Fusion Prompt Strategy, Fusion-modal Enhancing Prompt Strategy and Modality-aware and Stage-aware Prompt Strategy. To verify the effectiveness of these strategies, we conduct extensive ablation studies and analyses on RGBT234. In the experiments, we build a baseline tracker which does not contain any prompt strategies and is composed entirely of upstream parameters, with MFP replaced by an element-wise addition operation of dual-modal features. Based on the baseline, we explore the effectiveness of the prompt strategies we propose.

Uni-modal Exploration Prompt Strategy: We investigate the importance of the Uni-modal Exploration Prompt Strategy we propose. We apply this strategy alone to the baseline tracker and retrain the corresponding prompt word generation branch. As shown in Table 6, compared to the original tracker, the addition of the Uni-modal Exploration Prompt Strategy improves the PR and SR of the tracker on RGBT234 by 11.4 and 8.2 percentage points, respectively, which proves that this strategy significantly enhances

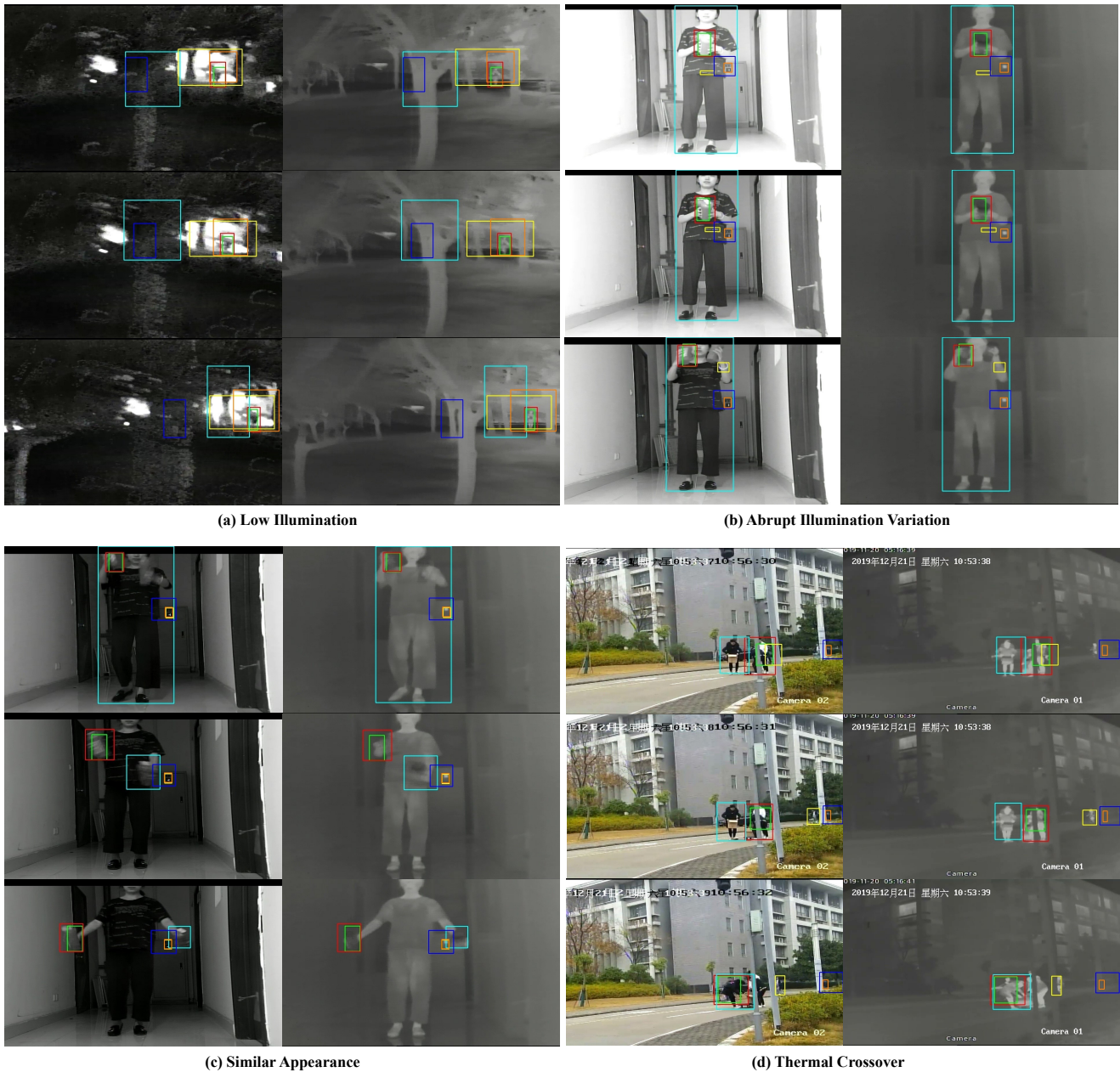


Figure 13: The qualitative evaluation results on the four most typical and challenging scenarios sampled. The green, red, cyan, yellow, blue, and orange bounding boxes are from the ground truth, our method, ViPT-deep, ProTrack, APFNet, and HMFT, respectively.

the adaptability of the first-stage backbone of foundation modal to the two uni-modal modeling tasks, and assists the backbone to fully explore the modality-shared features and modality-independent features.

Middle Fusion Prompt Strategy: To evaluate the impact of the Middle Fusion Prompt Strategy we propose, we replace the element-wise addition operation of the modal features in the original tracker with MFP, and provide fusion feature prompts for the second-stage backbone. According to the results in Table 10, the model with the Middle Fusion Prompt Strategy and retrained surpasses the original tracker

by 19.2 and 12.4 percentage points on the PR and SR metrics on RGBT234, respectively. This indicates that this prompt strategy can achieve adaptive selection of modal discriminative features, and provide reliable fusion feature prompts for the second-stage backbone.

Fusion-modal Enhancing Prompt Strategy: We also validate the proposed Fusion-modal Enhancing Prompting Strategy. Table 6 shows that this strategy boosts the PR and SR metrics of the original tracker on RGBT234 by 19.2 and 12.4 percentage points, respectively. This confirms that

our strategy better adapts the second-stage backbone to the fusion-modal modeling and feature enhancement.

Modality-aware and Stage-aware Prompt Strategy:

To evaluate the effectiveness and necessity of the Modality-aware and Stage-aware Prompt strategy we propose, we build a tracker that only contains the other three prompt strategies and a tracker that contains all four prompt strategies, and retrain them separately. According to the results in Table 6, although the collaboration of the three prompt strategies for different purposes has already achieved excellent performance on RGBT234, the Modality-aware and Stage-aware Prompt strategy still improves the PR and SR metrics by 1.4 and 1.2 percentage points, respectively. By storing only a small amount of parameters for the low-level fixed patterns within the modality, the strategy enables the foundation model to identify the current modality and sub-task faster and better, and achieves more robust tracking.

6. Conclusion

In this work, we propose a novel middle fusion framework for RGB-T tracking, which achieves a balance between performance and efficiency. We also design a new prompt tracking method based on this framework, using four flexible visual prompt strategies. These strategies not only maximize the use of upstream knowledge, but also fully exploit the potential of prompt learning in RGB-T tracking tasks. We evaluate our method on four challenging RGB-T tracking benchmarks, and show that it outperforms the current best prompt tracking method, and leads the existing RGB-T tracking methods, while maintaining a high efficiency. Moreover, we offer new insights for the exploration of visual prompt learning.

Acknowledgements

This work was supported in part by the National Natural Science Foundation of China under Grant 62273048.

References

- [1] Shitao Chen, Zhiqiang Jian, Yuhao Huang, Yu Chen, Zhuoli Zhou, and Nanning Zheng. Autonomous driving: cognitive construction and situation understanding. *Science China Information Sciences*, 62:1–27, 2019.
- [2] Hong Qiao, Shanlin Zhong, Ziyu Chen, and Hongze Wang. Improving performance of robots using human-inspired approaches: a survey. *Science China Information Sciences*, 65(12):221201, 2022.
- [3] Zixuan Xue and Wei Wu. Anomaly detection by exploiting the tracking trajectory in surveillance videos. *Science China Information Sciences*, 63:1–3, 2020.
- [4] Cheng Long Li, Andong Lu, Ai Hua Zheng, Zhengzheng Tu, and Jin Tang. Multi-adapter rgbt tracking. In *Proceedings of the IEEE/CVF International Conference on Computer Vision Workshops*, pages 0–0, 2019.
- [5] Lichao Zhang, Martin Danelljan, Abel Gonzalez-Garcia, Joost Van De Weijer, and Fahad Shahbaz Khan. Multi-modal fusion for end-to-end rgb-t tracking. In *Proceedings of the IEEE/CVF International Conference on Computer Vision Workshops*, pages 0–0, 2019.
- [6] Chenglong Li, Lei Liu, Andong Lu, Qing Ji, and Jin Tang. Challenge-aware rgbt tracking. In *Proceedings of the European Conference on Computer Vision*, pages 222–237. Springer, 2020.
- [7] Zhengzheng Tu, Chun Lin, Wei Zhao, Chenglong Li, and Jin Tang. M5: multi-modal multi-margin metric learning for rgbt tracking. *IEEE Transactions on Image Processing*, 31:85–98, 2021.
- [8] Andong Lu, Chenglong Li, Yuqing Yan, Jin Tang, and Bin Luo. Rgbt tracking via multi-adapter network with hierarchical divergence loss. *IEEE Transactions on Image Processing*, 30:5613–5625, 2021.
- [9] Pengyu Zhang, Jie Zhao, Chunjuan Bo, Dong Wang, Huchuan Lu, and Xiaoyun Yang. Jointly modeling motion and appearance cues for robust rgb-t tracking. *IEEE Transactions on Image Processing*, 30:3335–3347, 2021.
- [10] Tianlu Zhang, Xueru Liu, Qiang Zhang, and Jungong Han. Siam-cda: Complementarity-and distractor-aware rgb-t tracking based on siamese network. *IEEE Transactions on Circuits and Systems for Video Technology*, 32(3):1403–1417, 2021.
- [11] Yabin Zhu, Chenglong Li, Jin Tang, Bin Luo, and Liang Wang. Rgbt tracking by trident fusion network. *IEEE Transactions on Circuits and Systems for Video Technology*, 32(2):579–592, 2021.
- [12] Pengyu Zhang, Dong Wang, Huchuan Lu, and Xiaoyun Yang. Learning adaptive attribute-driven representation for real-time rgb-t tracking. *International Journal of Computer Vision*, 129:2714–2729, 2021.
- [13] Yun Xiao, Mengmeng Yang, Chenglong Li, Lei Liu, and Jin Tang. Attribute-based progressive fusion network for rgbt tracking. In *Proceedings of the AAAI Conference on Artificial Intelligence*, volume 36, pages 2831–2838, 2022.
- [14] Qiang Zhang, Xueru Liu, and Tianlu Zhang. Rgb-t tracking by modality difference reduction and feature re-selection. *Image and Vision Computing*, 127:104547, 2022.
- [15] Pengyu Zhang, Jie Zhao, Dong Wang, Huchuan Lu, and Xiang Ruan. Visible-thermal uav tracking: A large-scale benchmark and new baseline. In *Proceedings of the IEEE/CVF Conference on Computer Vision and Pattern Recognition*, pages 8886–8895, 2022.
- [16] Jinyu Yang, Zhe Li, Feng Zheng, Ales Leonardis, and Jingkuan Song. Prompting for multi-modal tracking. In *Proceedings of the 30th ACM International Conference on Multimedia*, pages 3492–3500, 2022.
- [17] Jiawen Zhu, Simiao Lai, Xin Chen, Dong Wang, and Huchuan Lu. Visual prompt multi-modal tracking. In *Proceedings of the IEEE/CVF Conference on Computer Vision and Pattern Recognition*, pages 9516–9526, 2023.
- [18] Luca Bertinetto, Jack Valmadre, Joao F Henriques, Andrea Vedaldi, and Philip HS Torr. Fully-convolutional siamese networks for object tracking. In *Proceedings of the European Conference on Computer Vision Workshops*, pages 850–865. Springer, 2016.
- [19] Bo Li, Junjie Yan, Wei Wu, Zheng Zhu, and Xiaolin Hu. High performance visual tracking with siamese region proposal network. In *Proceedings of the IEEE/CVF Conference on Computer Vision and Pattern Recognition*, pages 8971–8980, 2018.
- [20] Bo Li, Wei Wu, Qiang Wang, Fangyi Zhang, Junliang Xing, and Junjie Yan. Siamrpn++: Evolution of siamese visual tracking with very deep networks. In *Proceedings of the IEEE/CVF Conference on Computer Vision and Pattern Recognition*, pages 4282–4291, 2019.
- [21] Goutam Bhat, Martin Danelljan, Luc Van Gool, and Radu Timofte. Learning discriminative model prediction for tracking. In *Proceedings of the IEEE/CVF International Conference on Computer Vision*, pages 6182–6191, 2019.
- [22] Dongyan Guo, Jun Wang, Ying Cui, Zhenhua Wang, and Shengyong Chen. Siamcar: Siamese fully convolutional classification and regression for visual tracking. In *Proceedings of the IEEE/CVF Conference on Computer Vision and Pattern Recognition*, pages 6269–6277, 2020.
- [23] Xin Chen, Bin Yan, Jiawen Zhu, Dong Wang, Xiaoyun Yang, and Huchuan Lu. Transformer tracking. In *Proceedings of the IEEE/CVF Conference on Computer Vision and Pattern Recognition*, pages 8126–8135, 2021.
- [24] Bin Yan, Houwen Peng, Jianlong Fu, Dong Wang, and Huchuan Lu. Learning spatio-temporal transformer for visual tracking. In *Proceedings of the IEEE/CVF International Conference on Computer Vision*, pages 10448–10457, 2021.

- [25] Ziang Cao, Changhong Fu, Junjie Ye, Bowen Li, and Yiming Li. Hift: Hierarchical feature transformer for aerial tracking. In *Proceedings of the IEEE/CVF International Conference on Computer Vision*, pages 15457–15466, 2021.
- [26] Liting Lin, Heng Fan, Zhipeng Zhang, Yong Xu, and Haibin Ling. Swintrack: A simple and strong baseline for transformer tracking. In *Advances in Neural Information Processing Systems*, volume 35, pages 16743–16754, 2022.
- [27] Botao Ye, Hong Chang, Bingpeng Ma, Shiguang Shan, and Xilin Chen. Joint feature learning and relation modeling for tracking: A one-stream framework. In *Proceedings of the European Conference on Computer Vision*, pages 341–357. Springer, 2022.
- [28] Yutao Cui, Cheng Jiang, Limin Wang, and Gangshan Wu. Mixformer: End-to-end tracking with iterative mixed attention. In *Proceedings of the IEEE/CVF Conference on Computer Vision and Pattern Recognition*, pages 13608–13618, 2022.
- [29] Boyu Chen, Peixia Li, Lei Bai, Lei Qiao, Qiuqiang Shen, Bo Li, Weihao Gan, Wei Wu, and Wanli Ouyang. Backbone is all your need: A simplified architecture for visual object tracking. In *Proceedings of the European Conference on Computer Vision*, pages 375–392. Springer, 2022.
- [30] Kaijie He, Canlong Zhang, Sheng Xie, Zhixin Li, and Zhiwen Wang. Target-aware tracking with long-term context attention. *arXiv preprint arXiv:2302.13840*, 2023.
- [31] Yidong Cai, Jie Liu, Jie Tang, and Gangshan Wu. Robust object modeling for visual tracking. In *Proceedings of the IEEE/CVF International Conference on Computer Vision*, pages 9589–9600, 2023.
- [32] Lianghua Huang, Xin Zhao, and Kaiqi Huang. Got-10k: A large high-diversity benchmark for generic object tracking in the wild. *IEEE Transactions on Pattern Analysis and Machine Intelligence*, 43(5):1562–1577, 2021.
- [33] Heng Fan, Liting Lin, Fan Yang, Peng Chu, Ge Deng, Sijia Yu, Hexin Bai, Yong Xu, Chunyuan Liao, and Haibin Ling. Lasot: A high-quality benchmark for large-scale single object tracking. In *Proceedings of the IEEE/CVF Conference on Computer Vision and Pattern Recognition*, pages 5374–5383, 2019.
- [34] Matthias Muller, Adel Bibi, Silvio Giancola, Salman Alsubaihi, and Bernard Ghanem. Trackingnet: A large-scale dataset and benchmark for object tracking in the wild. In *Proceedings of the European conference on computer vision*, pages 300–317, 2018.
- [35] Chenglong Li, Wanlin Xue, Yaqing Jia, Zhichen Qu, Bin Luo, Jin Tang, and Dengdi Sun. Lasher: A large-scale high-diversity benchmark for rgbt tracking. *IEEE Transactions on Image Processing*, 31:392–404, 2021.
- [36] Menglin Jia, Luming Tang, Bor-Chun Chen, Claire Cardie, Serge Belongie, Bharath Hariharan, and Ser-Nam Lim. Visual prompt tuning. In *Proceedings of the European Conference on Computer Vision*, pages 709–727. Springer, 2022.
- [37] Amir Bar, Yossi Gandelsman, Trevor Darrell, Amir Globerson, and Alexei Efros. Visual prompting via image inpainting. *Advances in Neural Information Processing Systems*, 35:25005–25017, 2022.
- [38] Qidong Huang, Xiaoyi Dong, Dongdong Chen, Weiming Zhang, Feifei Wang, Gang Hua, and Nenghai Yu. Diversity-aware meta visual prompting. In *Proceedings of the IEEE/CVF Conference on Computer Vision and Pattern Recognition*, pages 10878–10887, 2023.
- [39] Kihyuk Sohn, Huiwen Chang, José Lezama, Luisa Polania, Han Zhang, Yuan Hao, Irfan Essa, and Lu Jiang. Visual prompt tuning for generative transfer learning. In *Proceedings of the IEEE/CVF Conference on Computer Vision and Pattern Recognition*, pages 19840–19851, 2023.
- [40] Alexey Dosovitskiy, Lucas Beyer, Alexander Kolesnikov, Dirk Weissenborn, Xiaohua Zhai, Thomas Unterthiner, Mostafa Dehghani, Matthias Minderer, Georg Heigold, Sylvain Gelly, et al. An image is worth 16x16 words: Transformers for image recognition at scale. In *International Conference on Learning Representations*, pages 0–0, 2020.
- [41] Ashish Vaswani, Noam Shazeer, Niki Parmar, Jakob Uszkoreit, Llion Jones, Aidan N Gomez, Lukasz Kaiser, and Illia Polosukhin. Attention is all you need. In *Advances in Neural Information Processing Systems*, volume 30, pages 6000–6010, 2017.
- [42] Tianlu Zhang, Hongyuan Guo, Qiang Jiao, Qiang Zhang, and Jungong Han. Efficient rgb-t tracking via cross-modality distillation. In *Proceedings of the IEEE/CVF Conference on Computer Vision and Pattern Recognition*, pages 5404–5413, 2023.
- [43] Chenglong Li, Xinyan Liang, Yijuan Lu, Nan Zhao, and Jin Tang. Rgb-t object tracking: Benchmark and baseline. *Pattern Recognition*, 96:106977, 2019.
- [44] Chenglong Li, Liang Lin, Wangmeng Zuo, and Jin Tang. Learning patch-based dynamic graph for visual tracking. In *Proceedings of the AAAI Conference on Artificial Intelligence*, volume 31, pages 1856–1864, 2017.
- [45] Seyed Morteza Ghazali and Yasser Baleghi. Rgbt tracking based on prior least absolute shrinkage and selection operator and quality aware fusion of deep and handcrafted features. *Knowledge-Based Systems*, page 110683, 2023.
- [46] Yabin Zhu, Chenglong Li, Jin Tang, and Bin Luo. Quality-aware feature aggregation network for robust rgbt tracking. *IEEE Transactions on Intelligent Vehicles*, 6(1):121–130, 2020.
- [47] Yabin Zhu, Chenglong Li, Bin Luo, Jin Tang, and Xiao Wang. Dense feature aggregation and pruning for rgbt tracking. In *Proceedings of the 27th ACM International Conference on Multimedia*, pages 465–472, 2019.
- [48] Andong Lu, Cun Qian, Chenglong Li, Jin Tang, and Liang Wang. Duality-gated mutual condition network for rgbt tracking. *IEEE Transactions on Neural Networks and Learning Systems*, pages 1–14, 2022.
- [49] Mingzheng Feng and Jianbo Su. Learning reliable modal weight with transformer for robust rgbt tracking. *Knowledge-Based Systems*, 249:108945, 2022.
- [50] Ruichao Hou, Tongwei Ren, and Gangshan Wu. Mirnet: A robust rgbt tracking jointly with multi-modal interaction and refinement. In *IEEE International Conference on Multimedia and Expo (ICME)*, pages 1–6. IEEE, 2022.
- [51] Matej Kristan, Jiri Matas, Ales Leonardis, Michael Felsberg, Roman Pflugfelder, Joni-Kristian Kamarainen, Luka ˇCehovin Zajc, Ondrej Drbohlav, Alan Lukezic, Amanda Berg, et al. The seventh visual object tracking vot2019 challenge results. In *Proceedings of the IEEE/CVF international conference on computer vision workshops*, pages 0–0, 2019.
- [52] Yuan Gao, Chenglong Li, Yabin Zhu, Jin Tang, Tao He, and Futian Wang. Deep adaptive fusion network for high performance rgbt tracking. In *Proceedings of the IEEE/CVF International Conference on Computer Vision Workshops*, pages 0–0, 2019.